Theory of two-dimensional microcavity lasers

Takahisa Harayama,[1] Satoshi Sunada,[1,2] and Kensuke S. Ikeda[2]

[1]*Department of Nonlinear Science, ATR Wave Engineering Laboratories, 2-2-2 Hikaridai Seika-cho Soraku-gun, Kyoto 619-0288, Japan*
[2]*Department of Physics Ritsumeikan University, 1-1-1 Noji-cho Kusatsu, Shiga 525-0577, Japan*

We present theoretical models of two-dimensional (2D) microcavity lasers. The relation between stationary lasing modes and resonances or metastable states is elucidated for arbitrary shapes of 2D resonant microcavities.

PACS number(s): 42.55.Sa, 42.65.Sf, 05.10.−a, 05.45.Mt

I. INTRODUCTION

Various kinds of devices, such as lasers and musical instruments, utilize stationary-wave oscillations in resonant cavities. In order to maintain stationary oscillation in these devices, nonlinearity is essential in the mechanism for balancing the pumping of the external energy and the decay of the wave of the quasistable state in the resonant cavity. Besides, the interaction between nonlinearities and the morphology of the boundary condition imposed on a resonating wave system by the shape of the cavity is also very important for determining the modes of oscillation [1,2].

Musical instruments sometimes have complex shapes in order to realize beautiful sounds in great variety [3]. On the other hand, one-dimensional (1D) simple shapes have been used for laser cavities because they are suitable for fabrication as well as for the application of directional emission. However, recent advances in the processing technology of dry etching for semiconductor laser diodes have made it possible to fabricate 2D microcavity lasers of arbitrary 2D shapes with potential applications for the 2D emission of laser light in optical communications and optical integrated circuits.

In particular, from the perspective of applications of small lasers in optical integrated circuits as well as fundamental physics, there has been much interest in 2D microdisks, which are circular symmetric and can confine light very efficiently by total internal reflection. Lasing in whispering gallery modes has been realized in microdisks [4–10].

It has been proposed that directional output can be obtained from 2D microcavity lasers by slightly deforming the circular geometry. The behavior of such a deformed cavity laser has been described in terms of the linear optical properties of the cavities, including chaotic ray optics and wave chaos [11]. In conventional nonchaotic laser cavities, such as Fabry-Perot, ring lasers, or microdisk lasers, there is a correspondence between each resonant mode and a quasiperiodic ray trajectory inside the cavity. For example, a whispering gallery mode in a microdisk laser corresponds to a quasiperiodic ray trajectory undergoing multiple reflections at shallow angles along the cavity walls. In a weakly deformed microdisk the cavity is weakly chaotic, and all ray trajectories eventually hit the edge of the cavity at an angle large enough for light to escape.

Another cavity shape has been proposed to obtain higher output power and more directional output from a "flattened quadrupole," which requires greater deformation of the disk shape [12]. This cavity shape has a "bow-tie" mode corresponding to a stable periodic ray trajectory which arises from reflections at four particular locations on the perimeter that provide a confocal resonator. Although these deformed microdisk lasers are partially chaotic, it is possible to describe the relation between shape and the optical confinement of low-loss modes in terms of ray trajectories.

The conventional theoretical approach to obtaining lasing modes in the above integrable or partially chaotic 2D microcavity laser is twofold [5,6,11–15]. First, the resonance scattering states are obtained by solving for the quasieigenmodes of the Helmholtz equation with appropriate boundary conditions and no active medium inside the cavity. Second, the angle of reflection for the eikonal rays corresponding to the resonance states is compared with the critical angle for total internal reflection to identify which modes have low loss.

In fully chaotic cavities, however, no stable ray trajectories exist, and there is typically no simple relation between ray trajectories and optical modes [16,17]. Moreover, rigorously speaking, the resonance state obtained by solving the Helmholtz equations is not a lasing state—it is typically not even a steady state but a quasistationary state with a complex frequency, which means that the solution is decaying. A nonlinear treatment, accounting for the nonlinearity of the polarization due to the lasing medium, is required to determine the existence of true steady states of lasing sustained by external pumping [18,19].

Furthermore, when more than one eigenmode of 2D microcaviy lasers are within the gain spectrum of the pumping, we cannot say from just the linear theory which modes will actually lase and which will not. Although we might expect that the microcavity will lase in the mode or modes closest to the gain center, this may not always be true. A fully nonlinear dynamical treatment is necessary to describe the actual lasing states of the 2D microcavity and the dynamical properties, such as growth at the onset of lasing, stabilities, saturation, and intermode interactions. Therefore, understanding the dynamics of lasing and lasing modes in 2D resonant microcavities remains an important challenge.

The conventional theory of 1D lasers is based on the expansion of the electromagnetic field by modes which are obtained as bound states by an approximation of the boundary condition by the closed cavity [18,19]. These modes are orthonormal and can expand arbitrary wave functions.

However, laser cavities are open systems where only resonances or quasistable states exist as eigenstates of which the

eigenfrequencies are complex instead of stable bound eigen-states of real eigenfrequencies [20]. It is not clear whether the approximation by a closed cavity works even in the case of 2D microcavity lasers, because they are quite different from 1D lasers in the sense that the light can be emitted from 2D edges in all directions of the plane.

Actually, it has been pointed out that the resonances play important roles in the description of 2D lasers [21,22]. How-ever, even the resonances cannot describe 2D microcavity lasers completely, because the lasing states are produced by the nonlinear interaction between the light field and the ac-tive lasing medium, and differ from the resonances that are the solutions of the linear Helmholtz equation without the active lasing medium.

In this paper, we present a nonlinear theory of 2D micro-cavity lasers described by including the effect of the active medium without any kind of modal description. We also elu-cidate the relation between the lasing modes and the reso-nances, and derive a model suitable for intuitive physical consideration by analogy with the Schrödinger equation as well as for numerical simulation. This model makes it pos-sible to simulate long-time dynamical behaviors of 2D mi-crocavity lasers.

Our paper is composed of six sections: In Sec. II, we derive the Maxwell-Bloch equations for 2D microcavity la-sers. Numerical results of the dynamical simulation of single-mode lasing in the microstadium resonant cavity are shown in Sec. III. In Sec. IV, we present another model for 2D microcavity lasers, which we call the Schrödinger-Bloch (SB) approach. The locking of two modes in 2D microcavity lasers is investigated by this method in Sec. V. Conclusions are contained in Sec. VI.

II. ELECTROMAGNETIC WAVES INTERACTING WITH TWO-LEVEL ATOMS

A. Maxwell equations

It is assumed that the waveguide is wide in the xy direc-tions and thin in the z direction. The refractive index sud-denly changes on the edge of the cavity. It is important to note that the light field affects the states of the atoms inside the cavity, and the states of the atoms also affect the light field. Such an interaction between the light field and the me-dium as well as the boundary condition reflecting the shape of the 2D microcavity laser combine together to produce the stationary lasing modes.

The electromagnetic fields E and H are described by the Maxwell equation with the polarization field P depending on the nonlinear response of the lasing medium:

$$\nabla \times E = -\frac{1}{c}\frac{\partial B}{\partial t}, \tag{1}$$

$$\nabla \cdot D = 0, \tag{2}$$

$$\nabla \times H = \frac{1}{c}\frac{\partial D}{\partial t}, \tag{3}$$

$$\nabla \cdot B = 0, \tag{4}$$

where

$$D = \varepsilon E + 4\pi P, \tag{5}$$

$$B = \mu H. \tag{6}$$

In the above, D is the electric displacement and B the magnetic induction.

We omit the dependence of the z direction of the electro-magnetic field. Therefore, Eqs. (1) and (3) are reduced to

$$\frac{\partial E_z}{\partial y} = -\frac{\mu}{c}\frac{\partial H_x}{\partial t}, \tag{7}$$

$$-\frac{\partial E_z}{\partial x} = -\frac{\mu}{c}\frac{\partial H_y}{\partial t}, \tag{8}$$

$$\frac{\partial E_y}{\partial x} - \frac{\partial E_x}{\partial y} = -\frac{\mu}{c}\frac{\partial H_z}{\partial t}, \tag{9}$$

$$\frac{\partial H_z}{\partial y} = \frac{1}{c}\frac{\partial}{\partial t}(\varepsilon E_x + 4\pi P_x), \tag{10}$$

$$-\frac{\partial H_z}{\partial x} = -\frac{1}{c}\frac{\partial}{\partial t}(\varepsilon E_y + 4\pi P_y), \tag{11}$$

$$\frac{\partial H_y}{\partial x} - \frac{\partial H_x}{\partial y} = \frac{1}{c}\frac{\partial}{\partial t}(\varepsilon E_z + 4\pi P_z). \tag{12}$$

When $H_z(E_z)$ vanishes, $E_x(H_x)$ and $E_y(H_y)$ should be zero. Accordingly, the solutions of Eqs. (7)–(12) are separated into TM-wave ($H_z=0$) and TE-wave ($E_z=0$) solutions. Conse-quently, we obtain

$$\frac{\partial^2}{\partial t^2}\left(E_z + \frac{4\pi}{\varepsilon}P_z\right) = \frac{c^2}{n^2}\nabla_{xy}^2 E_z - 2\beta\frac{\partial E_z}{\partial t}, \tag{13}$$

for the TM-wave solution, and

$$\frac{\partial^2}{\partial t^2}H_z = \frac{c^2}{n^2}\nabla_{xy}^2 H_z + \frac{4\pi c}{n^2}\left(\frac{\partial}{\partial y}P_x - \frac{\partial}{\partial x}P_y\right) - 2\beta\frac{\partial H_z}{\partial t}, \tag{14}$$

for the TE-wave solution, where β is introduced phenomeno-logically in order to represent the background absorption. In the above, n denotes the refractive index and equals $\varepsilon\mu$.

B. Two-level atoms

In order to describe the lasing medium, we use the well-known two-level medium model described by the optical Bloch equations

$$\frac{\partial}{\partial t}\rho = -i\omega_0\rho - i\kappa WE - \gamma_\perp\rho, \tag{15}$$

$$\frac{\partial}{\partial t}W = -2i\kappa E(\rho - \rho^*) - \gamma_\parallel(W - W_\infty), \tag{16}$$

where ρ and W are microscopic polarization and population inversion, respectively. In the above, ω_0 is the transition fre-

quency of the two-level medium, κ represents coupling strength, and the two relaxation parameters $\gamma_\perp$ and $\gamma_\parallel$ are the transversal relaxation rate and the longitudinal relaxation rate, respectively. W_∞ is the external pumping parameter.

The macroscopic polarization $\boldsymbol{P}$ is described with the microscopic polarization ρ as follows:

$$\boldsymbol{P} = N(\rho + \rho^*)\kappa\hbar\boldsymbol{e}, \qquad (17)$$

where N is the atomic number density and $\boldsymbol{e}$ is the unit vector parallel to the electric field $\boldsymbol{E}$.

C. Maxwell-Bloch equations

In the previous subsections, we have obtained the fundamental equations describing the electromagnetic fields and the active lasing medium. The electromagnetic fields evolve according to the Maxwell equations, which affect the states of two-level atoms according to the optical Bloch equations. The change of the active medium consisting of two-level atoms in turn affects the electromagnetic fields through the polarization term in the Maxwell equation. These interactions between the electromagnetic fields and the active lasing medium finally produce the stable lasing states.

From Eqs. (13) and (15)–(17), we finally obtain the Maxwell-Bloch equations for the TM-wave solution,

$$\frac{\partial^2}{\partial t^2}\left(E_z + \frac{4\pi}{\varepsilon}P_z\right) = \frac{c^2}{n^2}\nabla_{xy}^2 E_z - 2\beta\frac{\partial E_z}{\partial t}, \qquad (18)$$

$$P_z = N(\rho + \rho^*)\kappa\hbar, \qquad (19)$$

$$\frac{\partial}{\partial t}\rho = -i\omega_0\rho - i\kappa W E_z - \gamma_\perp\rho, \qquad (20)$$

$$\frac{\partial}{\partial t}W = -2i\kappa E_z(\rho - \rho^*) - \gamma_\parallel(W - W_\infty). \qquad (21)$$

From Eqs. (10), (11), and (14)–(17), we also obtain the Maxwell-Bloch equations for the TE-wave solution,

$$\frac{\partial^2}{\partial t^2}H_z = \frac{c^2}{n^2}\nabla_{xy}^2 H_z + \frac{4\pi c}{n^2}\frac{\partial}{\partial t}\left(\frac{\partial}{\partial y}P_x - \frac{\partial}{\partial x}P_y\right) - 2\beta\frac{\partial H_z}{\partial t}, \qquad (22)$$

$$\frac{1}{c}\frac{\partial}{\partial t}(\varepsilon E_x + 4\pi P_x) = \frac{\partial H_z}{\partial y}, \qquad (23)$$

$$\frac{1}{c}\frac{\partial}{\partial t}(\varepsilon E_y + 4\pi P_y) = -\frac{\partial H_z}{\partial x}, \qquad (24)$$

$$P = N(\rho + \rho^*)\kappa\hbar\boldsymbol{e}, \qquad (25)$$

$$\frac{\partial}{\partial t}\rho = -i\omega_0\rho - i\kappa W E - \gamma_\perp\rho, \qquad (26)$$

$$\frac{\partial}{\partial t}W = -2i\kappa E(\rho - \rho^*) - \gamma_\parallel(W - W_\infty). \qquad (27)$$

The above model does not include the effect of spontaneous emission although it is important to discuss laser applications such as coherence and quantum noise.

D. Stationary Maxwell-Bloch equations for single-mode lasing

Here, we show that the Maxwell-Bloch equations can be reduced to more simple time-independent equations when laser action occurs only on a single mode.

1. TM-wave solution

Let us suppose that the electric field oscillates with frequency ω as $E_z = E_s(x,y)e^{-i\omega t} + E_s^*(x,y)e^{i\omega t}$. Because of the rotating-wave approximation (RWA), it can be assumed that the polarization has the following form: $\rho = -i\rho_s(x,y)e^{-i\omega t}$. Then from Eq. (18) we have

$$\left(\nabla_{xy}^2 + n^2\frac{\omega^2}{c^2}\right)E_s = i4\pi\mu N\kappa\hbar\frac{\omega^2}{c^2}\rho_s - 2i\beta\omega E_s. \qquad (28)$$

By substituting E_s and ρ into the Bloch equations (20) and (21), and by applying the RWA, we obtain

$$\rho_s = \frac{\kappa E_s}{\gamma_\perp + i(\omega_0 - \omega)}W_s \qquad (29)$$

and

$$W_s = \frac{W_\infty}{1 + \xi_\omega|E_s|^2}, \qquad (30)$$

where

$$\xi_\omega \equiv \frac{\dfrac{4\kappa^2}{\gamma_\perp\gamma_\parallel}}{1 + (\omega_0 - \omega)^2/\gamma_\perp^2}. \qquad (31)$$

From Eqs. (28)–(30), we finally obtain the equation for the stationary lasing of the TM-wave solution,

$$\left(\nabla_{xy}^2 + n^2\frac{\omega^2}{c^2}\right)E_s = i\zeta\frac{\omega^2}{c^2}L(\omega)\left(1 + i\frac{\omega - \omega_0}{\gamma_\perp}\right)\frac{W_\infty}{1 + \xi_\omega|E_s|^2}E_s$$
$$- 2i\beta\omega E_s, \qquad (32)$$

where $\zeta \equiv 4\pi N\mu\kappa^2\hbar$. In the above, $L(\omega)$ denotes the Lorentzian gain function—i.e.,

$$L(\omega) \equiv \frac{\gamma_\perp}{(\omega - \omega_0)^2 + \gamma_\perp^2}. \qquad (33)$$

From the Maxwell equation, we have the boundary condition of the electric field as follows: $E_{s,in} = E_{s,out}$ and $(\partial/\partial n)E_{s,in} = (\partial/\partial n)E_{s,out}$, where $E_{s,in}$ and $E_{s,out}$ are the electric fields inside and outside the 2D microcavity, respectively, and $\partial/\partial n$ denotes the normal derivative to the edge of the cavity [23]. The right-hand side of Eq. (32) represents the effects of the gain and absorption due to the presence of the lasing medium, and hence it should vanish outside the cavity. Instead, the radiative-wave condition should be satisfied outside the cavity because no mechanism exists for reflecting the waves outside the cavity.

2. TE-wave solution

In the same way as for the TM-wave solution, we can assume that the electromagnetic fields and polarization for the TE-wave solution oscillate with frequency ω as $H_z = H_s(x,y)e^{-i\omega t} + H_s(x,y)^* e^{i\omega t}$, $\boldsymbol{E} = \{E_s(x,y)e^{-i\omega t} + E_s(x,y)^* e^{i\omega t}\}\boldsymbol{e}$, and $\rho = -i\rho_s(x,y)e^{-i\omega t}$. Then we can obtain the polarization

$$
\begin{aligned}
\boldsymbol{P} &= N\kappa\hbar(-i\rho_s e^{-i\omega t} + i\rho_s e^{i\omega t})\boldsymbol{e} \\
&= -iN\kappa^2\hbar W_s\left(\frac{e^{-i\omega t}}{\gamma_\perp + i(\omega_0 - \omega)}E_s \right.\\
&\left. + \frac{e^{i\omega t}}{\gamma_\perp - i(\omega_0 - \omega)}E_s^*\right)\boldsymbol{e}.
\end{aligned}
\tag{34}
$$

Consequently, from Eq. (22) we finally obtain the equation for the stationary lasing of the TE-wave solution,

$$
\begin{aligned}
\left(\nabla_{xy}^2 + n^2\frac{\omega^2}{c^2}\right)H_s = &-\frac{\zeta}{\mu}\frac{\omega}{c}L(\omega)\left(1 + i\frac{\omega - \omega_0}{\gamma_\perp}\right)\left(\frac{\partial}{\partial y}(W_s E_x)\right. \\
&\left. - \frac{\partial}{\partial x}(W_s E_y)\right) - 2i\beta\omega H_s.
\end{aligned}
\tag{35}
$$

From the Maxwell equation, we have the boundary condition of the magnetic field as follows: $H_{s,in} = H_{s,out}$, and $(\partial/\partial n)H_{s,in} = (1/n_{in}^2)(\partial/\partial n)H_{s,out}$, where $H_{s,in}$ and $H_{s,out}$ are the magnetic fields inside and outside the 2D microcavity, respectively [23]. In the above, n_{in} is the refractive index inside the cavity. Outside the cavity, the right-hand side of Eq. (35) vanishes, and the radiative-wave condition should be satisfied.

E. Linear stationary Maxwell-Bloch equations

When the pumping power is just above the lasing threshold, the higher-order terms of the electromagnetic fields can be neglected. Therefore, from Eq. (32) we obtain the linear stationary Maxwell-Bloch equations

$$
\left(\nabla_{xy}^2 + n^2\frac{\omega^2}{c^2}\right)E_s = i\zeta\frac{\omega^2}{c^2}L(\omega)\left(1 + i\frac{\omega - \omega_0}{\gamma_\perp}\right)W_\infty E_s - 2i\beta\omega E_s.
\tag{36}
$$

The boundary conditions of the TM-wave solution are imposed. Outside the cavity, the right-hand side of Eq. (36) vanishes, and the resonance wave function should satisfy the radiative-wave condition.

Next, we show that the linearized stationary Maxwell-Bloch equation for the TE-wave solution has the same form as the one for the TM-wave solution. From Eq. (23), we have

$$
\frac{\partial H_s}{\partial y} = -i\frac{\omega}{c}\left(\varepsilon - i4\pi N\kappa^2\hbar\frac{W_\infty}{\gamma_\perp + i(\omega_0 - \omega)}\right)E_{s,x}.
\tag{37}
$$

Assuming

$$
\varepsilon \gg i4\pi N\kappa^2\hbar\frac{W_\infty}{\gamma_\perp + i(\omega_0 - \omega)}
\tag{38}
$$

yields

$$
E_{s,x} = i\frac{c}{\omega\varepsilon}\frac{\partial H_z}{\partial y}, \quad E_{s,y} = -i\frac{c}{\omega\varepsilon}\frac{\partial H_z}{\partial x}.
\tag{39}
$$

Accordingly, from Eq. (35) we obtain

$$
\begin{aligned}
\left(\nabla_{xy}^2 + \frac{n^2}{c^2}\omega^2\right)H_s = &-i\frac{4\pi N\kappa^2\hbar}{\varepsilon}\frac{W_\infty}{\gamma_\perp + i(\omega_0 - \omega)}\nabla_{xy}^2 H_s \\
&- 2i\beta\omega H_s.
\end{aligned}
\tag{40}
$$

From inequality (38), we finally obtain

$$
\left(\nabla_{xy}^2 + n^2\frac{\omega^2}{c^2}\right)H_s = i\zeta\frac{\omega^2}{c^2}L(\omega)\left(1 + i\frac{\omega - \omega_0}{\gamma_\perp}\right)W_\infty H_s - 2i\beta\omega H_s.
\tag{41}
$$

The boundary conditions of the TE-wave solution are imposed. The right-hand side of Eq. (41) vanishes and the resonance-wave function should satisfy the radiative-wave condition outside the cavity.

Consequently, the linear Maxwell-Bloch equations of the TM- and TE-wave solutions are of precisely the same form

$$
\left(\nabla_{xy}^2 + n^2\frac{\omega^2}{c^2}\right)U_s = i\zeta\frac{\omega^2}{c^2}L(\omega)\left(1 + i\frac{\omega - \omega_0}{\gamma_\perp}\right)W_\infty U_s - 2i\beta\omega U_s,
\tag{42}
$$

where U_s represents E_s and H_s, although the boundary conditions for the TM-wave and TE-wave solutions are different from each other. Outside the cavity, the right-hand side of Eq. (42) vanishes because of the lack of a lasing medium, and the wave function should satisfy the radiative-wave condition. When there is no external pumping—that is, $W_\infty = 0$—solutions of Eq. (42) are resonances which are quasistable states and of which the frequencies are complex. The real part of the complex resonance frequency ω_j corresponds to the oscillation frequency of the electromagnetic field, while the imaginary part of the complex resonance frequency ω_j is always negative and corresponds to the loss of the microcavity or the decay rate of the resonance.

As the external pumping power is increased, the position of the resonance frequency in the complex plane becomes closer to the real axis because the decay rate of the resonance decreases. The effect of the active gain medium and the background absorption is expressed as the right-hand side of Eq. (42), where the oscillation frequency in the gain function of the first term of Eq. (42) is a real number. If the resonance frequency is not far from the real axis, the effect of the active gain medium on the resonance can be estimated by substituting the real part of the complex resonance frequency. Accordingly, the shifted resonance frequency ω_j' due to the presence of the linear gain can be expressed approximately by the original resonance ω_j of no pumping power,

$$
\omega_j'^2 = \omega_j^2 + \zeta\frac{\text{Re }\omega_j^2}{c^2}L(\text{Re }\omega_j)\left(\frac{\text{Re }\omega_j - \omega_0}{\gamma_\perp} + i\right)W_\infty - 2i\beta\omega_j.
\tag{43}
$$

Therefore we obtain the lasing condition for the resonance ω_j from the imaginary part of ω_j',

$$\frac{\zeta}{2}\frac{\mathrm{Re}\ \omega_j}{c^2}L(\mathrm{Re}\ \omega_j)W_\infty > -\mathrm{Im}\ \omega_j + \beta. \qquad (44)$$

On the threshold of lasing, the pumping power balances with the loss of the microcavity and the resonance reaches the real axis. Therefore, from Eq. (43), we obtain the frequency shift on the threshold,

$$\omega_j' = \frac{(-\mathrm{Im}\ \omega_j + \beta)\omega_0 + \gamma_\perp\ \mathrm{Re}\ \omega_j}{(-\mathrm{Im}\ \omega_j + \beta) + \gamma_\perp}. \qquad (45)$$

It is important to note that the lasing frequency ω_j' becomes closer to the gain center ω_0 as the decay rate of the resonance increases.

Below the lasing threshold of the pumping power, the frequencies of the resonance of the linear Maxwell-Bloch equation (42) have a negative imaginary part, and hence its wave function is divergent outside the cavity. On the other hand, the wave function of the resonance of Eq. (42) is not radiative above the lasing threshold because the imaginary part of the resonance is positive. Accordingly, the resonance solutions of the linear Maxwell-Bloch equation (42) below and above the lasing threshold are not appropriate for the lasing solutions. Only just on the lasing threshold does the frequency of the resonance solution of Eq. (42) become real, and its wave function satisfies the radiative-wave condition outside the 2D microcavity. Consequently, the solution of the linear Maxwell-Bloch equation (42) just on the lasing threshold very well approximates the stationary lasing state of single-mode lasing.

III. DYNAMICAL SIMULATION OF MICROSTADIUM LASERS

The approximation of the linear description for single-mode lasing in the previous section is correct only when the light field is weak. Besides, as the pumping power is increased, more than one resonance mode obtains positive gains, and how a resonance mode behaves asymptotically is answered only by the full nonlinear dynamical simulation of the Maxwell-Bloch equations (18)–(27).

In our simulation we chose a stadium [24] for the cavity shape consisting of two half circles and two flat lines, as shown by the white curve in Fig. 1. The stadium shape, known as Bunimovich's stadium, is well known as a shape which can be exactly proven to be fully chaotic, and it has been a popular model in research on classical and quantum chaos.

The radius of the half circles of the stadium R =0.365 μm and the length of the horizontal lines equals $2R$. We set the refractive indexes inside and outside the stadium to n_{in}=3.3 and n_{out}=1, respectively. The other parameters are reported to be as follows: $\gamma_\parallel$=6.6×10^{12} s^{-1}, $\gamma_\perp$ =1.1×10^{13} s^{-1}, ε=n^2, μ=1, β=8.8×10^{12} s^{-1}, N =4.3×10^{18} cm^{-3}, κ=1.1×10^{15} s^{-1}, $\hbar$=6.62621×10^{-34} J s, ω_0=2.2×10^{15} s^{-1}, and $N \times W_\infty$=4.3×10^{15} cm^{-3}.

We simulated the time evolution of the light field of the TM-wave solution subject to Eqs. (18)–(21), starting from an initial condition of the Gaussian wave packet shown in Fig. 1. In order to carry out a dynamical simulation, we used the
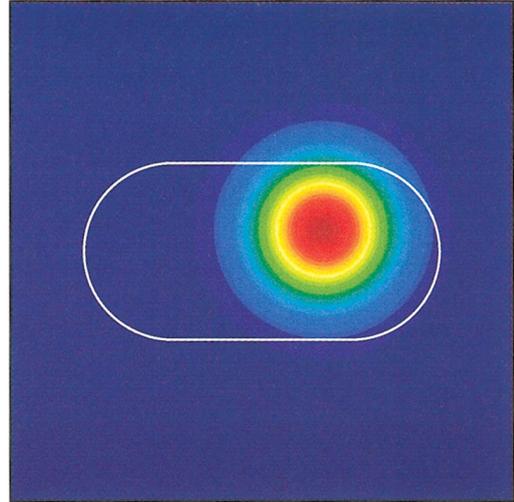

FIG. 1. (Color) The initial state of the light field. The final stationary lasing state does not depend on the initial state. The white curve denotes the stadium cavity.

finite-difference time-domain method. The details of the numerical computation will be discussed elsewhere.

The total light intensity inside the stadium is small at first; however, it grows exponentially and saturates to oscillate with a constant frequency. In Fig. 2, we show the power spectrum of the time evolution of the light field in the time region after the saturation. The single sharp peak means that single-mode lasing occurs.

We calculated the distribution of the resonances, which are the solutions of the linear Maxwell-Helmholtz equation for the cold cavity. The resonances obtained by the extended boundary element method are shown in Fig. 3 [25]. The single and double circles in Fig. 3 satisfy the lasing condition (44), while the crosses correspond to the resonances that do not satisfy (44). The sharp peak in Fig. 2 precisely corresponds to the real part of the resonance frequency of the double circle in Fig. 3. Therefore, we conclude that the laser action occurs on the resonance marked by the double circle in Fig. 3.

Indeed, the spatial wave function of the final stable oscillation state obtained by the dynamical simulation of the Maxwell-Bloch equations (18)–(21) shown in Fig. 4 excel-
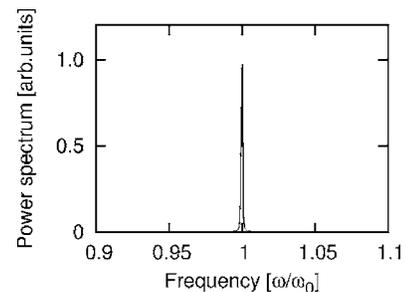

FIG. 2. The power spectrum obtained from the time evolution of the light field in the time region of a stable oscillation. The oscillation frequency corresponds well to that of the resonance denoted by the double circle in Fig. 1.
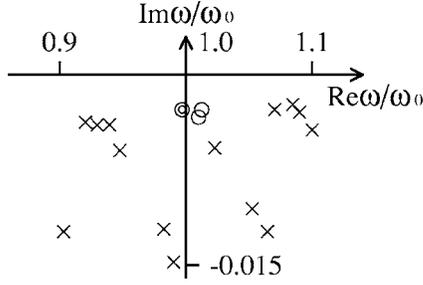
FIG. 3. Resonances of a microstadium cavity. The double and single circles correspond to the resonances of the maximum and second maximum gain.

lently corresponds to the wave function of the resonance mode marked by the double circle in Fig. 3 shown in Fig. 5, which is obtained by the extended boundary element method. Therefore, we conclude that only the resonance mode marked by the double circle in Fig. 3 wins the mode competition with the other resonance modes and can lase. It is interesting that no closed ray trajectories correspond to the lasing mode in Fig. 4.

IV. SCHRöDINGER-BLOCH APPROACH

The linear Maxwell-Bloch equations for 2D microcavity lasers of an arbitrary shape can be solved numerically—for example, by the boundary element method. The solution of the linear Maxwell-Bloch equations for the pumping power just on the threshold nicely approximates the real lasing states just above the threshold. However, the approximation of the linear Maxwell-Bloch equations becomes worse as the pumping power increases. Moreover, the interactions among resonance modes cannot be investigated by the linear Maxwell-Bloch equations.

Consequently, the time-dependent full-order Maxwell-Bloch equations must be solved in order to investigate 2D microcavity lasers with high pumping power. It takes a very long time to simulate the dynamics of 2D microcavity lasers
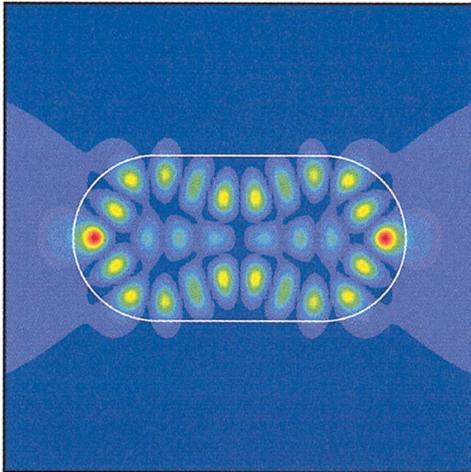
by solving numerically the full-order Maxwell-Bloch equations that we have derived in the previous sections. However, this method is inefficient for a study on the dynamics of lasing because the fast oscillation as well as the slowly varying envelope of the light field are simulated.

It is important to note that the fast oscillation part of the light field has the constant frequency ω_s, which is very close to the transition frequency ω_0 of the two-level medium. Accordingly, it is possible to separate the slowly varying part from the fast oscillation part in order to investigate the dynamics of 2D microcavity lasers efficiently. In this section, we propose an efficient method to investigate the dynamics of the slowly varying part of the TM wave [26]. This method enables us to simulate very long-time behavior of 2D microcavity lasers and to investigate the interactions among resonance modes.

Let us suppose $\widetilde{E}$ and $\widetilde{\rho}$ to be the slowly varying envelope of the electric field and the polarization field as $E_z = e^{-i\omega_s t}\widetilde{E}(x,y;t) + e^{i\omega_s t}\widetilde{E}^*(x,y;t)$ and $\rho = -ie^{-i\omega_s t}\widetilde{\rho}(x,y;t)$, where the RWA is taken into consideration for the polarization. Applying the slowly varying envelope approximation for time to Eq. (18) yields the following equation for the electric field inside the cavity:

$$\frac{\partial}{\partial t}\widetilde{E} = \frac{i}{2}(\nabla_{xy}^2 + 1)\widetilde{E} - \alpha_L\widetilde{E} + \frac{2\pi N\kappa\hbar}{\varepsilon}\widetilde{\rho}, \qquad (46)$$

where space and time are made dimensionless by the scale transformation $(n_{in}\omega_s/c)x$, $(n_{in}\omega_s/c)y \rightarrow (x,y)$, $t\omega_s \rightarrow t$, respectively, and $\alpha_L \equiv \beta/\omega_s$. From Eqs. (20) and (21), the Bloch equations are also transformed,

$$\frac{\partial}{\partial t}\widetilde{\rho} = -\widetilde{\gamma}_\perp\widetilde{\rho} - i\Delta_0\widetilde{\rho} + \widetilde{\kappa}W\widetilde{E} \qquad (47)$$

and

FIG. 4. (Color) The final stationary lasing state. It oscillates with the peak frequency shown in Fig. 3.
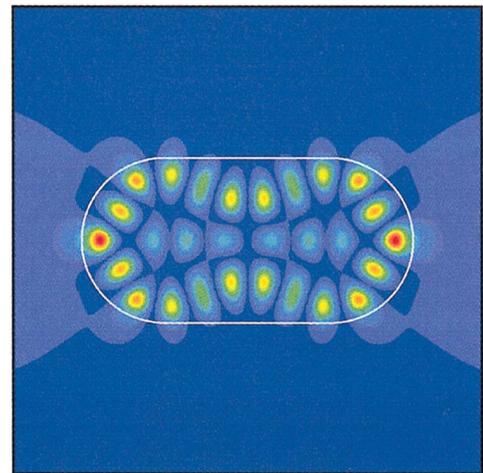

FIG. 5. (Color) The wave function of the resonance of the double circle in Fig. 1. It excellently corresponds to the final stationary lasing state shown in Fig. 3.
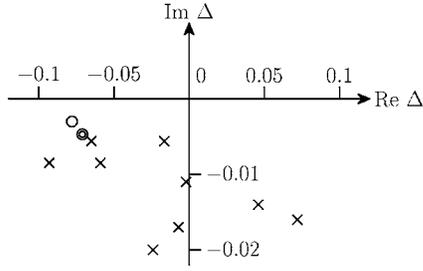
FIG. 6. Resonances of a microstadium cavity. The double and single circles correspond to the resonances of the maximum and second maximum gain.

$$\frac{\partial}{\partial t}W = -\tilde{\gamma}_\parallel(W - W_\infty) - 2\tilde{\kappa}(\tilde{E}\tilde{\rho}^* + \tilde{E}^*\tilde{\rho}), \qquad (48)$$

where the dimensionless parameters are defined as follows: $\tilde{\gamma}_\perp \equiv \gamma_\perp/\omega_s$, $\tilde{\gamma}_\parallel \equiv \gamma_\parallel/\omega_s$, $\tilde{\kappa} \equiv \kappa/\omega_s$, and $\Delta_0 \equiv [\omega_0 - \omega_s]/\omega_s$.

In the same way, we have the equation for the electric field outside the cavity:

$$\frac{n_{out}^2}{n_{in}^2}\frac{\partial}{\partial t}\tilde{E} = \frac{i}{2}\left(\nabla_{xy}^2 + \frac{n_{out}^2}{n_{in}^2}\right)\tilde{E}. \qquad (49)$$

Here one encounters difficulty in applying one of the most efficient methods for simulating of the wave propagation, known as the split-operator method (or symplectic-integrator method), to Eqs. (46) and (49). Therefore, we assume Eq. (49) can be approximated by

$$\frac{\partial}{\partial t}\tilde{E} = \frac{i}{2}\left(\nabla_{xy}^2 + \frac{n_{out}^2}{n_{in}^2}\right)\tilde{E}. \qquad (50)$$

Indeed, this approximation works very well when the difference of the refractive indexes between the inside and outside of the cavity is small.

Now, Eqs. (46) and (50) are just the Schrödinger equation with an additional nonlinear effect of polarization. The Laplacian term can be interpreted as the kinetic energy while the term of the refractive index is the potential energy. We shall refer to the set of equations (46)–(48) and (50) as the 2D SB model.

In introducing this SB model in this paper, we claim that the merits of the model are twofold: it allows us to use intuition from quantum mechanics to establish a physical picture of lasing, and it allows us to use techniques of the split-operator method (or symplectic-integrator method) to carry out numerical simulations of the nonlinear dynamics of 2D microcavity lasers [27].

It is enough to investigate the SB model for a qualitative observation of the nonlinear dynamical behavior of 2D microcavity lasers, although the Maxwell-Bloch equations should be used for quantitative estimation of the lasing characteristics. A detailed discussion of the approximation of the SB model by using microdisk lasers will be reported elsewhere.

Next we derive the equation for single-mode lasing in the case of the SB model. Assuming the stationary oscillation of the electric and polarization fields, respectively, $\tilde{E} = \tilde{E}_s e^{-i\Delta_s t}$ and
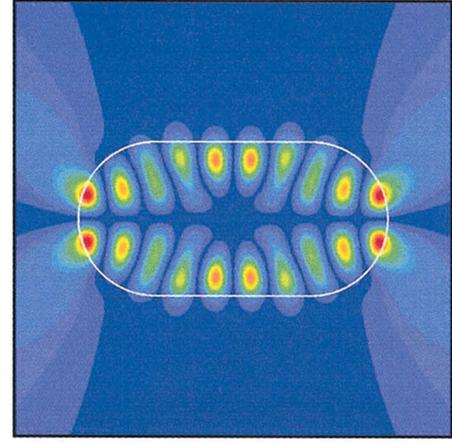
(a)
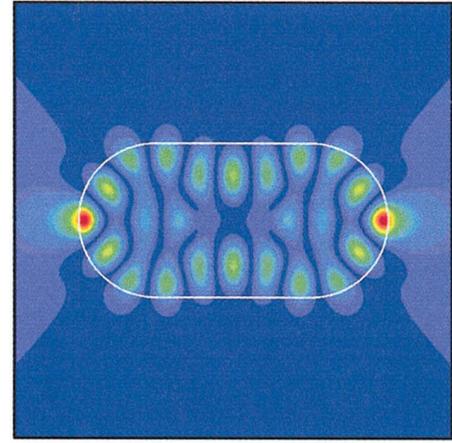
(b)

FIG. 7. (Color) The wave function of the resonance of (a) the double circle and (b) single circle in Fig. 1. These wave functions are solutions of the linear Schrödinger-Helmholtz equation. The symmetry classes of these modes are, respectively, (a) $\psi_{--}(x,y)$ and (b) $\psi_{++}(x,y)$. The white curve denotes the stadium cavity.

and $\tilde{\rho} = \tilde{\rho}_s e^{-i\Delta_s t}$, and the constant population inversion $W = W_s$ yields the time-independent SB equation in the same way as the stationary Maxwell-Bloch equations,

$$\left[\nabla^2 + \left(2\Delta_s + \frac{n^2}{n_{in}^2}\right)\right]\tilde{E}_s = 2i\alpha(\Delta_s)\frac{W_\infty}{1 + \eta(\Delta_s)|\tilde{E}_s|^2}\tilde{E}_s - 2i\alpha_L\tilde{E}_s, \qquad (51)$$

where the complex Lorentzian gain $\alpha(\Delta_s)$ and the strength of the nonlinearity $\eta(\Delta_s)$ are defined as follows:

$$\alpha(\Delta_s) \equiv \alpha_0 \frac{1}{\tilde{\gamma}_\perp^2 + (\Delta_s - \Delta_0)^2}[\tilde{\gamma}_\perp + i(\Delta_s - \Delta_0)] \qquad (52)$$
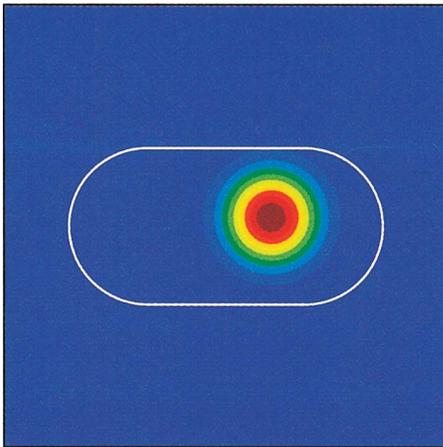
FIG. 8. (Color) The initial state of the light field. The final stationary state does not depend on the initial state. The white curve denotes the stadium cavity.

$$\eta(\Delta_s) \equiv \frac{4\widetilde{\kappa}^2}{\widetilde{\gamma}_\parallel \widetilde{\gamma}_\perp} \frac{\widetilde{\gamma}_\perp^2}{\widetilde{\gamma}_\perp^2 + (\Delta_0 - \Delta_s)^2}. \quad (53)$$

Here $\alpha_0 \equiv 2\pi N\kappa\widetilde{\kappa}\hbar/\varepsilon$.

The refractive index n in Eq. (51) equals n_{in} inside the cavity and n_{out} outside the cavity. The right-hand side of Eq. (51) represents the effect of the lasing medium and vanishes outside the cavity. The wave functions of the solution of Eq. (51) satisfy the boundary condition $\widetilde{E}_{s,in} = \widetilde{E}_{s,out}$ and $(\partial/\partial n)\widetilde{E}_{s,in} = (\partial/\partial n)\widetilde{E}_{s,out}$, where $\widetilde{E}_{s,in}$ and $\widetilde{E}_{s,out}$ are the slowly varying envelopes of the electric fields inside and outside the

FIG. 10. (Color) The final lasing state of the light field. The wave function corresponds to that of mode A as shown in Fig. 7(a).

2D microcavity, respectively, and $\partial/\partial n$ denotes the normal derivative to the edge of the cavity. The wave functions also satisfy the radiative-wave condition because there exist no reflective waves which propagate from outside to inside the cavity.

Equation (51) inherits the mechanism of the single-mode lasing of the stationary Maxwell-Bloch equation (32). Accordingly, one can obtain the condition for lasing: that is, the gain exceeds the loss. For this purpose, we linearize Eq. (51),

$$\left[\nabla^2 + \left(2\Delta_s + \frac{n^2}{n_{in}^2} \right) \right] \widetilde{E}_s = 2i\alpha(\Delta_s)W_\infty \widetilde{E}_s - 2i\alpha_L \widetilde{E}_s. \quad (54)$$
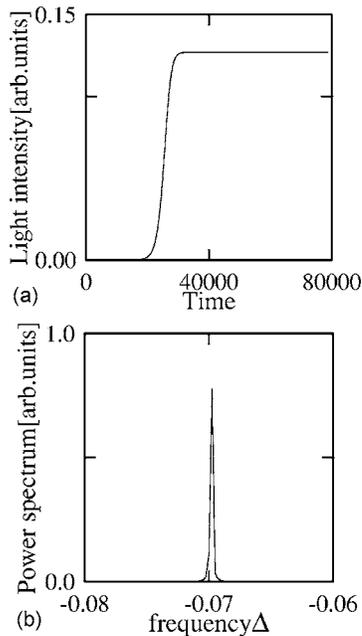

FIG. 9. (a) The light intensity inside the cavity vs time in the case of $W_\infty = 1.7 \times 10^{-4}$. The light intensity grows exponentially and saturates to be a constant. (b) The optical spectrum obtained from the time evolution of the light field in the time region of a stable oscillation. The peak corresponds to mode A.
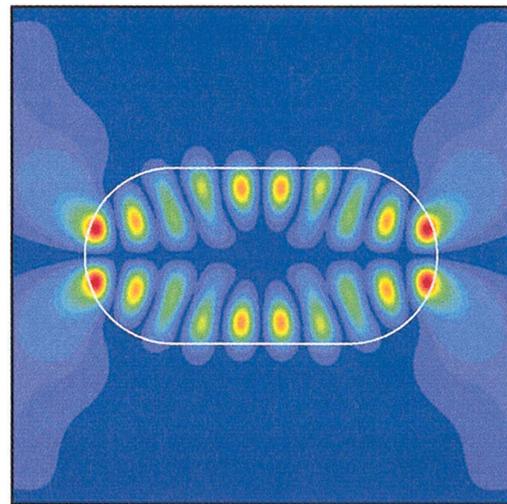

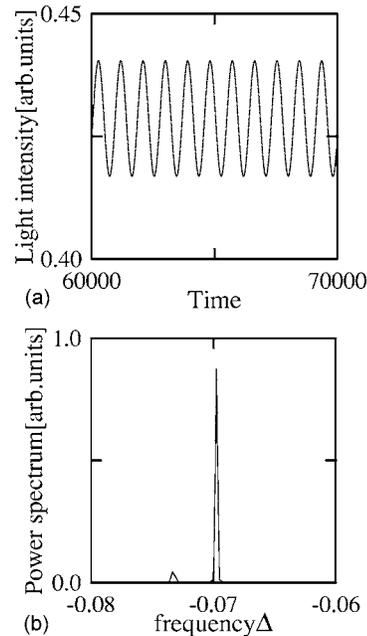FIG. 11. (a) The light intensity inside the cavity vs time in the case of $W_\infty = 2.0 \times 10^{-4}$. The time evolution of the light intensity is quasiperiodic. (b) The optical spectrum has two peaks. The higher peak frequency (ν_1) corresponds to mode A, and the other peak frequency (ν_2) corresponds to mode B.
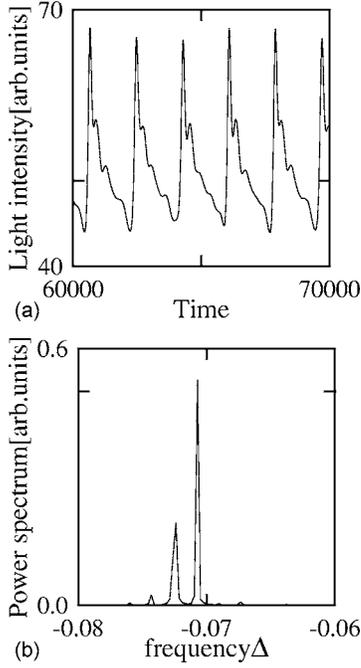
FIG. 12. (a) The light intensity inside the cavity vs time in the case of $W_\infty = 35 \times 10^{-4}$. The time evolution of the light intensity is the limit cycle. (b) The optical spectrum has two large peaks corresponding to modes A and B, respectively, and small peaks of the higher harmonics of the two large peaks frequencies.

First let us consider the case of no external pumping power—i.e., $W_\infty = 0$. Then we obtain the time-independent Schrödinger equation with the energy 2Δ and the potential $-n^2/n_{in}^2$. Therefore, there exist bound states in the region of $\Delta < -n^2/2n_{in}^2$. These bound states should be excluded from the lasing states by an appropriate setting of the gain center Δ_0 and the background absorption α_L because they are fictitious and come from the slowly varying envelope approximation. Thus, we can focus only on the resonances Δ_j as candidates for the final lasing states. In the same way as in the linear Maxwell-Bloch equation, we obtain the shifted resonance Δ_j' by a first-order correction due to the presence of the gain and absorption in Eq. (51),

$$\Delta_j' = \Delta_j - i\alpha_L + i\alpha(\mathrm{Re}\,\Delta_j)W_\infty. \tag{55}$$

When the gain term $\mathrm{Re}\,\alpha(\mathrm{Re}\,\Delta_j)W_\infty$ exceeds the total linear loss $-\mathrm{Im}\,\Delta_j + \alpha_L$, the corresponding mode grows exponentially and can lase. Consequently, we obtain the lasing condition for the resonance Δ_j,

$$\alpha_0 \frac{\widetilde{\gamma}_\perp W_\infty}{\widetilde{\gamma}_\perp^2 + (\Delta_0 - \mathrm{Re}\,\Delta_j)^2} > -\mathrm{Im}\,\Delta_j + \alpha_L. \tag{56}$$

Just on the lasing threshold of the pumping power, the shifted frequency at which imaginary part vanishes is given by
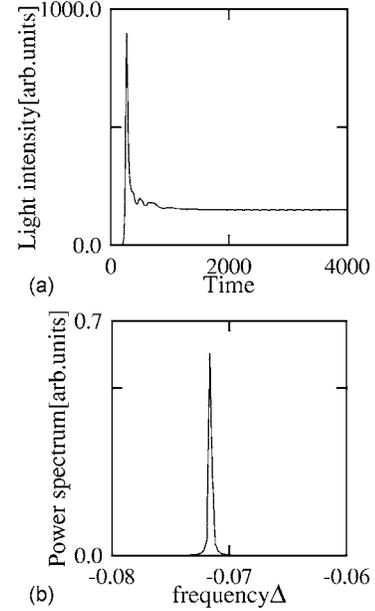

FIG. 13. (a) The light intensity inside the cavity vs time in the case of $W_\infty = 100 \times 10^{-4}$. The time evolution of the light intensity grows exponentially at first and exhibits a relaxation oscillation, at last becoming stationary. (b) The optical spectrum has only one peak due to the mode-locking phenomenon.

$$\Delta_j' = \frac{\widetilde{\gamma}_\perp\,\mathrm{Re}\,\Delta_j + (-\mathrm{Im}\,\Delta_j + \alpha_L)\Delta_0}{(-\mathrm{Im}\,\Delta_j + \alpha_L) + \widetilde{\gamma}_\perp}. \tag{57}$$

Therefore, the lasing frequency of the resonance of larger cavity loss is shifted from the original resonance frequency. It is important to note that the wave function of the resonance varies as the frequency is shifted. This is the simplest description of lasing in the SB picture. Notice that the lasing threshold for all bound-state modes (i.e., $\mathrm{Im}\,\Delta_j = 0$ modes) is the same and, moreover, the threshold of bound modes is just zero if there is no linear loss due to absorption.

Such a linear description is correct only when the field intensity is weak. How a mode behaves asymptotically, or how it dynamically interacts with other modes, is answered only by a fully nonlinear analysis of the SB equation. In order to carry out the numerical simulation, we used the symplectic integrator method for the Schrödinger equation and the Euler method for the Bloch equations. To check the validity of the results, we compared the results for the steady state with the solutions of the nonlinear eigenmode analysis for the Schrödinger-Bloch equations in our previous work.

V. DYNAMICAL SIMULATION BY SCHRÖDINGER-BLOCH MODEL

In this section, the effect of the nonlinear interaction between two resonance modes is investigated by using the Schrödinger-Bloch model. In Sec. III, nonlinear dynamical simulation of the Maxwell-Bloch model has shown that stable lasing in a fully chaotic cavity is possible in a spatially chaotic pattern of the light field of a resonance mode which is only a metastable state of a passive cavity without an
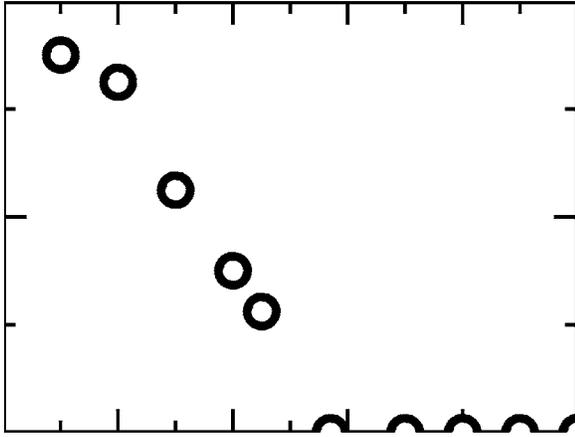
FIG. 14. The difference of the frequencies ν_1 and ν_2 corresponding to the two lasing modes decreases as the pumping power increases.

active gain medium in the cavity [8]. Accordingly, resonance solutions of the stationary linear Maxwell equation—i.e., the Helmholtz equation—in the passive 2D microcavities of arbitrary shapes can be identified as stationary lasing modes as long as the resonances are isolated in the complex wave number plane and multimode lasing does not occur. However, when the resonances are densely distributed in the complex wave number plane, multimode lasing occurs and modes interact with each other. In this case, the linear theory only solving the Helmholtz equation cannot predict the precise lasing characteristics because the nonlinear interaction among modes through an active medium plays a very important role. Especially, a nonlinear treatment is important for understanding mode locking, which is a typical nonlinear phenomenon of laser dynamics [18,19].

It is important to note that most of the 2D microcavities previously studied are symmetric with respect to the x and y axes, such as an elliptical cavity. The resonance modes are then divided into four symmetry classes: $\psi_{ab}(-x,y) = a\psi_{ab}(x,y)$ and $\psi_{ab}(x,-y) = b\psi_{ab}(x,y)$ with the parities $a \in \{+,-\}$ and $b \in \{+,-\}$. We show that when two modes of different symmetry classes are locked, the pattern of a stationary lasing state becomes asymmetric.

In our simulation we chose a stadium [24] for the cavity shape, consisting of two half circles of radius $R=49/4\sqrt{2} \approx 8.75$ and two flat lines of length $2R$, as shown in Fig. 2. We set the refractive index inside and outside the stadium to $n_{in}=2.0$ and $n_{out}=1$, respectively. The other parameters are reported to be as follows: $\tilde{\gamma}_{\parallel}=0.003$, $\tilde{\gamma}_{\perp}=0.006$, $\epsilon=4$, $\mu =1.0$, $\kappa=0.5$, $\alpha_L=0.004$, $N\kappa\hbar=1.0$, and $\Delta_0=-0.07$. We made all the quantities dimensionless. If we were to assume that the wavelength of the lasing mode is 0.86 μm, the length of the flat line of the stadium would be 1.2 μm. It is important that the Bunimovich's stadium billiard has a symmetric shape.

By using the extended the boundary element method, we solved the linear Schrödinger-Helmholtz equation under the boundary condition that the refractive index suddenly change on the edge of the cavity and there exist only radiative waves outside the cavity. The distribution of the resonances [8,25]

is shown in Fig. 6. The resonances denoted by the double circle and circle are close to the gain center $\Delta_0=-0.07$ and have long lifetimes. We call them modes A and B, respectively. The wave functions of modes A and B corresponding to these resonances are shown in Figs. 7(a) and 7(b). Modes A and B belong to different symmetry classes: Mode A belongs to $\psi_{--}(x,y)$ while mode B belongs to $\psi_{++}(x,y)$. The resonance wave functions are not bounded and spread beyond the edge of the cavity. Consequently the rate equation formalism cannot apply to this case, and the laser dynamics should be investigated by calculating full equations of the 2D Schrödinger-Bloch model.

First let us explain single-mode lasing on mode A. In order to carry out the dynamical simulation of the Schrödinger-Bloch model, we used the symplectic integrator method for the Schrödinger equation and the Euler method for the Bloch equations. The time evolution of the light field started from an initial condition of the Gaussian wave packet of the width 5.0 centered at the point (5.0,1.0) in a stadium shaped cavity as shown in Fig. 8, where the origin of the xy coordinates is the center of the stadium. When the pumping power W_∞ is smaller than $W_{sing}=1.5\times10^{-4}$, no stationary state exists and no lasing occurs in any modes. As the pumping power W_∞ is increased more than $W_{sing}=1.5\times10^{-4}$, the total light intensity inside the stadium grows exponentially and saturates to be a constant for arbitrary initial states as shown in Fig. 9(a). The optical spectrum has one peak corresponding to the real part of the resonant frequency as shown in Fig. 9(b). The wave function of the final stable state shown in Fig. 10 excellently corresponds to the wave function of mode A shown in Fig. 7(a). The other mode B does not have positive gain and cannot lase. Therefore, only mode A can lase in this region of W_∞.

Next we discuss two-mode lasing on modes A and B. These two resonance modes interact with each other through the active gain medium, and their different frequencies are pulled together, which is called "mode pulling." Mode-pulling phenomena here can be classified into quasiperiodic behaviors of 2D tori and limit cycles. When W_∞ is increased to more than $W_t=1.9\times10^{-4}$, mode B can also obtain enough gain to lase. When $W_t<W_\infty\leqslant W_l=1.0\times10^{-3}$, the interaction between modes A and B is small and hence the time evolution of the light field is quasiperiodic as if there exist two independent modes of different oscillation frequency ν_1 and ν_2, as shown in Fig. 11. As W_∞ is increases to be more than W_l, the interaction between modes A and B becomes larger. Consequently, the light field is attracted into a limit cycle as shown in Fig. 12(a). When $W_l<W_\infty\leqslant W_{lock}=5.6\times1.0^{-3}$, the optical spectrum has two large peaks at ν_1 and ν_2, respectively corresponding to modes A and B, and small peaks of their higher harmonics as shown in Fig. 12(b).

Finally we explain the locking of modes A and B induced by the strong coupling due to the nonlinear effect of the active medium inside the cavity. When $W_\infty>W_{lock}$, the total intensity of the light field inside the cavity grows exponentially at first and shows relaxation oscillation, and at last becomes stationary as shown in Fig. 13(a). Indeed, the optical spectrum has only one peak above this locking threshold as shown in Fig. 13(b). Figure 14 shows that the frequency difference $|\nu_1-\nu_2|$ decreases and vanishes at $W_\infty=W_{lock}$ as the pumping power increases.
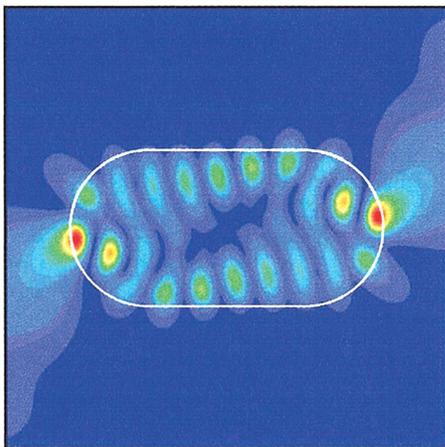
FIG. 15. (Color) The asymmetric pattern of the final stable oscillation of the light field.

The most important point of the locking of two modes in 2D microcavity lasers is that the final stationary lasing state has an asymmetric pattern as shown in Fig. 15, in spite of the cavity's symmetric shape. The asymmetric pattern is explained by the superposition of two different parity modes A and B with the same frequency due to the locking. We note that a reflection-symmetric pair of the patterns of Fig. 15 is also a stable stationary lasing state.

The asymmetric pattern of the light field does not change in the course of the time evolution, and hence the far-field pattern of the output light is also stationary and asymmetric. In addition, we have checked that the locking of two modes belonging to different symmetry classes is a universal phenomenon in 2D microcavity lasers of arbitrary shapes. Indeed, the asymmetric far-field pattern has actually been observed in a 2D semiconductor microcavity laser diode [28,29].

VI. CONCLUSION

We have presented two approaches to 2D microcavity lasers of arbitrary shapes. The Maxwell-Bloch model is precise, and thus it is useful for quantitative estimation and practical for the design of real 2D microcavity lasers, while the Schrödinger-Bloch model is useful for the qualitative investigation of the complex dynamical behaviors of the light field.

Laser action on a single spatially chaotic wave function is obtained as a final stable state by dynamical simulations of both models of a stadium-shaped resonant cavity. The stable single-mode lasing state corresponds to a particular metastable resonance of the cavity which wins in a competition among multiple modes with positive net linear gain and has a distinct lasing threshold.

Mode-pulling phenomena and the locking of two resonance modes of different symmetry classes and different frequencies in 2D microcavity lasers were investigated by dynamical simulation of the Schrödinger-Bloch model. The patterns of stationary lasing states and far fields are asymmetric in spite of the symmetric shape of the resonant microcavity.

[1] S. Adachi, J. Acoust. Soc. Am. **95**, 2912 (1994).

[2] T. Idogawa, T. Kobata, K. Komuro, and M. Iwaki, J. Acoust. Soc. Am. **93**, 540 (1993).

[3] N. H. Fletcher and T. D. Rossing, *The Physics of Musical Instruments* (Springer-Verlag, New York, 1998).

[4] Y. Yamamoto and R. E. Slusher, Phys. Today **46**(6), 66 (1993).

[5] *Optical Processes in Microcavities*, edited by R. K. Chang and A. J. Campillo (World Scientific, Singapore, 1996).

[6] S. L. McCall, A. F. J. Levi, R. E. Slusher, S. J. Pearton, and R. A. Logan, Appl. Phys. Lett. **60**, 289 (1992).

[7] M. Gonokami, K. Takeda, H. Yasuda, and K. Ema, Jpn. J. Appl. Phys., Part 2 **31**, L99 (1992).

[8] T. Harayama, P. Davis, and K. S. Ikeda, Phys. Rev. Lett. **82**, 3803 (1999).

[9] J. Faist, C. Gmachl, M. Striccoli, C. Sirtori, F. Capasso, D. L. Sivco, and A. Y. Cho, Appl. Phys. Lett. **69**, 2456 (1996).

[10] C. Gmachl, J. Faist, F. Capasso, C. Sirtori, D. L. Sivco, and A. Y. Cho, IEEE J. Quantum Electron. **33**, 1567 (1997).

[11] J. U. Nöckel and A. D. Stone, Nature (London) **385**, 45 (1997).

[12] C. Gmachl, F. Capasso, E. E. Narimanov, J. U. Nöckel, A. D. Stone, J. Faist, D. L. Sivco, and A. Y. Cho, Science **280**, 1556

(1998).

[13] S. Chang, R. K. Chang, A. D. Stone, and J. U. Nöckel, J. Opt. Soc. Am. B **17**, 1828 (2000).

[14] C. Gmachl, E. E. Narimanov, F. Capasso, J. N. Baillargeon, and A. Y. Cho, Opt. Lett. **27**, 824 (2002).

[15] S.-B. Lee, J.-H. Lee, J.-S. Chang, H.-J. Moon, S. W. Kim, and K. An, Phys. Rev. Lett. **88**, 033903-1 (2002).

[16] M. C. Gutzwiller, *Chaos in Classical and Quantum Mechanics* (Springer, Berlin, 1990).

[17] H. J. Stöckmann, *Quantum Chaos: An Introduction* (Cambridge University Press, Cambridge, England, 1999).

[18] M. Sargent III, M. O. Scully, and W. E. Lamb, Jr., *Laser Physics* (Addison-Wesley, Reading, MA, 1974).

[19] M. P. Meystre and M. Sargent III, *Elements of Quantum Optics* (Springer-Verlag, Berlin, 1990).

[20] A. E. Siegman, Appl. Phys. B: Lasers Opt. **60**, 247 (1995).

[21] C. Viviescas and G. Hackenbroich, Phys. Rev. A **67**, 013805 (2003).

[22] E. S. C. Ching, P. T. Leung, A. Maassen van den Brink, W. M. Suen, S. S. Tong, and K. Young, Rev. Mod. Phys. **70**, 1545 (1998).

[23] John David Jackson, *Classical Electrodynamics*, 3rd ed.

(Wiley, New York, 1998).

[24] L. A. Bunimovich, Commun. Math. Phys. **65**, 295 (1979).

[25] J. Wiersig, J. Opt. A, Pure Appl. Opt. **5**, 53 (2003).

[26] T. Harayama, P. Davis, and K. S. Ikeda, Phys. Rev. Lett. **90**, 063901 (2003).

[27] K. Takahashi and K. S. Ikeda, J. Chem. Phys. **106**, 4463

(1997).

[28] T. Harayama, T. Fukushima, S. Sunada, and K. S. Ikeda, Phys. Rev. Lett. **91**, 073903 (2003).

[29] T. Fukushima, T. Harayama, T. Miyasaka, and P. O. Vaccaro, J. Opt. Soc. Am. B **21**, 935 (2004).